



Journal of Applied Sciences

ISSN 1812-5654

science
alert

ANSI*net*
an open access publisher
<http://ansinet.com>

Nonlinear Analysis of Reinforced Concrete Beams Under Pure Torsion

Mohammad Najim Mahmood
Department of Civil Engineering, Mosul University, Mosul, Iraq

Abstract: A nonlinear finite element analysis is conducted using ANSYS-V10 finite element package on six reinforced concrete cantilever beams having different length vary from 0.5 to 3 m with 0.5 m increments and subjected to a concentrated torque at the free end. The beams are designed to carry the same torque. The study emphasize on the effect of beam length (span to depth ratio) on the torsional strength and behavior of reinforced concrete rectangular beams and the effectiveness of the torsional reinforcement in the pre and post cracking stages of loading. It was found that beams with span/depth ratio equal to or more than 4 have the same reserved torsional strength and less than those with smaller ratio, keeping the cross section and torsional reinforcements constant for all the beams. Before cracking stresses in transverse and longitudinal reinforcement are almost negligible and it is far below the yield stress even at the post cracking stages. Reinforcement attained yielding only at ultimate torque and after the wide spread of cracks in the shorter beam.

Key words: ANSYS, beam, concrete, nonlinear, reinforcement, torsion

INTRODUCTION

Understanding the response of reinforced concrete beam under pure torsion is crucial due to the fact that the elastic theory is not applicable for reinforced concrete composite material. The nonlinear finite element analysis may be one of the best solutions for this type of problem. There is an immense work in the field of nonlinear finite element analysis of reinforced concrete structures (William and Tanabe, 2001). The work concerning the study of the torional behavior of reinforced concrete beams using nonlinear finite element method is very limited; on the contrary; a lot of experimental and theoretical works based on either elastic or plastic theory have been done in this area (Hsu, 1968; Fang and Shiau, 2004). The effects of longitudinal reinforcement on the torsional capacity of rectangular beams under combined torsion and moment are found to be marginal through the experimental work done by Aryal (2005) and Rahal (2000). Recently, Hao-Jan *et al.* (2006) experimentally investigated the effects of aspect ratio of the cross section and the variation of volume ratio of transverse to longitudinal reinforcement on the cracking and ultimate strength of reinforced rectangular concrete beams under pure torsion. The effect of the span on torsional behavior of reinforced concrete beam has not been yet investigated. So the present work is an attempt to predict the nonlinear response of cantilever reinforced concrete rectangular beam under pure torsion using the finite element package

ANSYS-V10 (2005) aiming to predict the effect of the span of cantilever beam on its torsional response and the safety margin in the (ACI318-05, 2005) code provisions, highlight the effectiveness of the torsional reinforcement in the pre and post cracking stages of rectangular reinforced concrete beams under pure torsion, predict variation of the stresses in the transverse and longitudinal torsional reinforcements at different stages of loading. Six cantilever beams with different length varies from 0.5 to 3 m with 0.5 m increments are analyzed under torsional moment applied at the free end of the beam. The cross section, longitudinal and transverse reinforcement are kept constant for all the beams and this is the main limitations of the present study.

DETAILS OF THE BEAMS

The six cantilever beams has been assigned the notations, B1, B2, B3, B4, B5 and B6 having span of 0.5, 1, 1.5, 2, 2.5 and 3 m length, respectively. Each beam is reinforced with 10 mm bar diameter (area = 79 mm²) vertical closed stirrups spaced at 150 mm center to center and 6Φ12 (area = 113 mm² each) longitudinal reinforcement bars. These are the required torsional reinforcement for the beam as per the (ACI318-05) design code to carry a factored torque (Tu) equal to 23 kN.m using concrete cylinder strength (f_c) equal to 30 MPa with steel yield strength (f_y) equal to 400 MPa. Since the cantilever beam is statically determinant structure, the torque will be

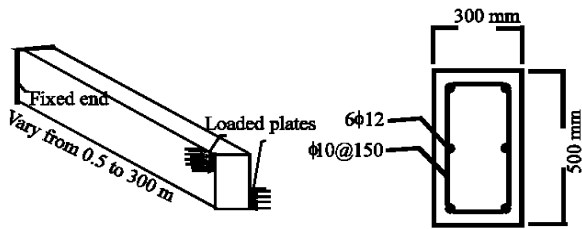


Fig. 1: Details of the analyzed Beam

constant along the span and the required torsional reinforcements are constant along the span and identical for the six beams. The details of the adopted cross section and arrangement of loading are shown in Fig. 1.

FINITE ELEMENT MODELLING

Three different types of element are used to model each of the reinforced concrete beams; the first one is the Solid65 concrete brick element which is used for 3D modeling of concrete with or without reinforcing bars (rebar). This element has eight nodes with three degrees of freedom per node-translations in the global x, y and z directions. The element is capable of handling plastic deformation, cracking in three orthogonal directions and crushing. It has also the ability to model the reinforcement as equivalent smeared within the element with the proper orientation. The adopted element size is 50×50×50 mm such that the number of Solid65 concrete elements used for B1 to B6 beams are 600, 1200, 1800, 2400, 3000 and 3600 elements, respectively. The second element type is the Solid45 brick element used for the loading steel plate, which is used to avoid local failure of concrete at the load locations. Each plate is 150 mm depth, 100 mm width and 30 mm thick modeled by 6 Solid45 elements. These plates located at the two staggered opposite sides of the beam free end as shown in Fig. 1. Equal load with opposite direction is uniformly applied over these two plates to develop the required torsion. The third element type is the Link8 element which was used to model the steel reinforcement. This element is a 3D spar element and it has two nodes with three translational degrees of freedom per node. This element is also capable of handling plastic deformation and is used to represent the steel bars. The length of each Link8 element is 50 mm perfectly connected to the nodes of the concrete element. Mesh for beam B6 is shown in Fig. 2, in which some of the concrete elements are removed to show the steel elements.

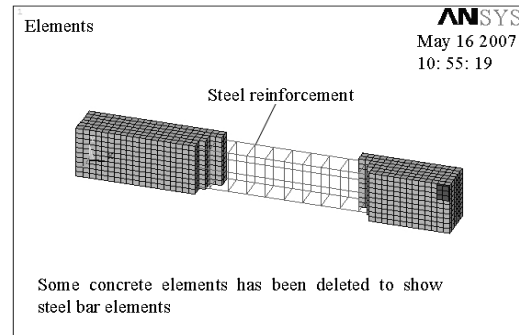


Fig. 2: Finite element mesh for beam B6

MATERIALS MODELS

Concrete: ANSYS software has the ability to model different types of material properties. Cracking of concrete and stress-strain relation in tension is modelled by a linear elastic tension stiffening relationship. The cracking stress of concrete is taken equal to the modulus of rupture calculated according to the (ACI318-05) code and it is equal to 3.5 MPa. In the present study the ability of concrete to transfer shear forces across the crack interface is accounted for by using two different shear retention factor (β) for cracked shear modulus, it was assumed equal to 0.3 for opened crack and 0.7 for closed crack. The concrete constitutive relationships under multiaxial state of stresses, is based upon the William and Warnke (1975) model which are considered as an appropriate model to describe the concrete failure. In this model the yield condition is approximated by five parameters and it is used to distinguish linear from non-linear and elastic from inelastic deformations using the failure envelope defined by a scalar function of stress $f(\sigma) = 0$ through a flow rule, using incremental stress-strain relations. The author present the equivalent uniaxial stress-strain relationship for the concrete under compression by using the equation suggested by Desayi and Krishnan (1964) to compute the multilinear isotropic stress-strain curve for the concrete (Mac Gregor, 1992) in the form:

$$\sigma = \frac{E_c \varepsilon}{1 + \left(\frac{\varepsilon}{\varepsilon_0} \right)^2} \quad (1)$$

Where, E_c is the elastic modulus of concrete calculated as per the (ACI318-05) code and it is equal to 26017MPa for $f_c = 30$ MPa, ε strain corresponding to stress σ and ε_0 is

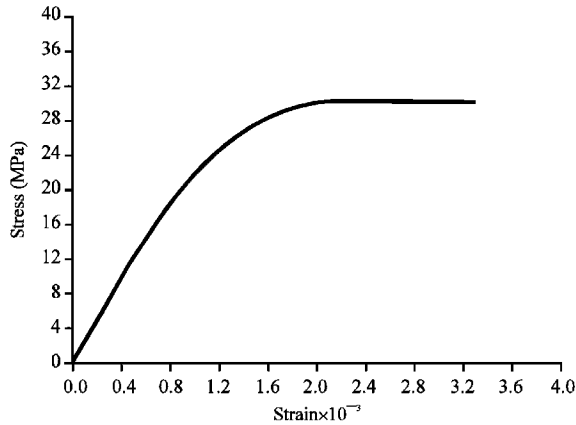


Fig. 3: Multilinear stress-strain isotropic hardening curve for concrete

the strain at peak stress equal to $(2f_c/E_c)$ and f_c is the concrete compressive strength. Ten points are used to represent the stress strain curve using Eq. 1 starting from the elastic stress limit ($0.3f_c$) up to $f_c = 30$ MPa and last point is corresponding to ultimate strain (ϵ_u) equal to 0.003 at peak stress $f_c = 30$ MPa. The resulting multilinear isotropic hardening stress-strain curve for concrete is shown in Fig. 3.

Steel: In the present study a Bilinear Kinematics Hardening (BKIN) is adopted for steel bars and loading plates. The yield stress is equal to 400 MPa and the hardening modulus is taken equal to 200 MPa; while the elastic modulus is equal to 200000 MPa and Poisson's ratio 0.3.

RESULTS AND DISCUSSION

Each of the six beams is analyzed under increasing incremental torque equal to 0.5 kN.m up to failure. The torque is induced by a uniform load applied over the staggered opposite plate at the free end of the beam. The ultimate load is assumed to be reached when the solution is not converged. The predicted variations of twist angle with the applied torque for all the beams are shown in Fig. 4, which shows that ductility of the beams in the post cracking stages is significantly increased by increasing the length of the beam.

The predicted cracking torque (T_{cr}), elastic torque (T_e), ultimate torque (T_u) and the percent safety margin (reserved strength) over the design torque (23 kN.m) are shown Table 1, where (T_e) is the torque that limits the linear part of the torque-twist curve. The Table 1 also contains comparison between the predicted elastic torsional stiffness (K_e) and that based on beam theory

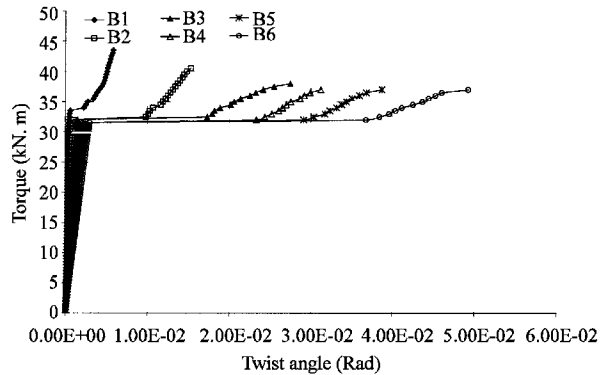


Fig. 4: Torque-twist angle for the analyzed beams

Table 1: Predicted cracking, elastic and ultimate torque and safety margin

Beam No.	T_{cr} (kN.m)	T_e (kN.m)	T_u (kN.m)	Safety (%)	K_e (kN.m rad ⁻¹)	GJ/L (kN.m rad ⁻¹)
B1	26	34.5	43.5	89	90156	60548
B2	24	32.5	41.0	78	36232	30274
B3	23	32.0	38.5	67	22831	20183
B4	22	31.5	37.5	63	16681	15137
B5	22	31.5	37.5	63	13138	12110
B6	22	31.5	37.5	63	10835	10091

(GJ/L), where (K_e) represent the initial slope (linear part) of the torque-twist curve, G is shear modulus, J is the torsional rigidity which for these beams cross section is equal to (0.002795 m^3) and L is the span of the beam. The ultimate torque shown in Table 1 is the torque at which divergence occurred. It is clear that the predicted torsional stiffness (K_e) for B1 is about 50% greater than that calculated by the elastic theory and the difference get reduced for beams with longer span and it becomes 7% for the longer beam B6. The Table 1 also shows that the cracking and ultimate torques for beam B1 (having span/depth ratio equal to 1) is about 17% more than that of B4, B5 and B6 which have same failure torque (37.5 kN.m).

It can be seen that the three values of the torque (T_u , T_e and T_{cr}) are reduced by increasing the span from 0.5 to 2 m and these values become constant for the beams having span equal to or more than 2 m (Fig. 5). Thus it can be stated that, when the span to depth ratio is equal to or more than 4, the span has no effect on the torsional strength of cantilever beam under pure torsion.

Figure 6 and 7 show a sample of the crack pattern of beam B2 at torque level $T_e = 31.5$ kN.m and at 32 kN.m, respectively. These two figures show the drastic change in the rotation of the beam and the wide spread of the cracks along the span when the torque exceeds the (T_e) value by only 0.5 kN.m increment. Cracks are first started at the vicinity of the loaded plate as shown in Fig. 6, then these cracks are widely spread along the span of the beam

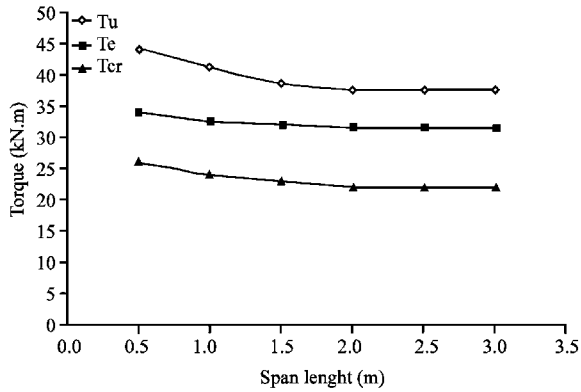


Fig. 5: Variations of Tu, Te and Tcr with the span of cantilever

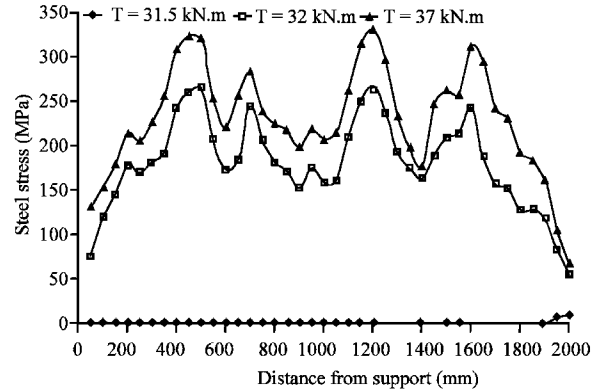


Fig. 8: Variation of longitudinal steel stress at mid depth along span of beam B4

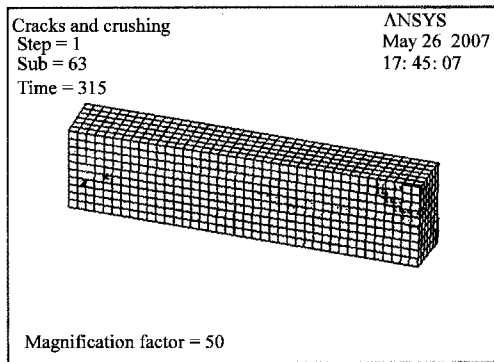


Fig. 6: Crack pattern for B4 at torque equal to 31.5 kN.m

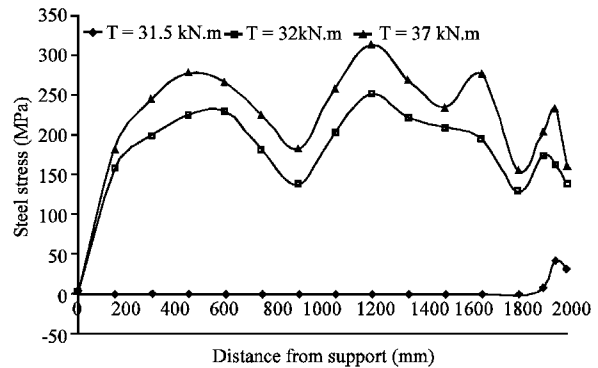


Fig. 9: Variation of stress at mid depth of stirrups along the span of beam B4

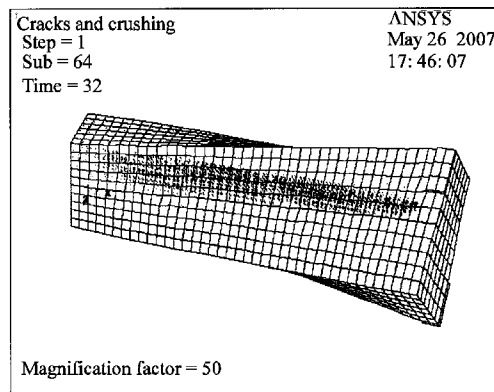


Fig. 7: Crack pattern for B4 at torque equal to 32 kN.m

at torque equal to 32 kN.m as shown in Fig. 7. This explains the sudden change in the twist angle when the torque exceeds (T_e) for all the beams as shown in Fig. 4.

To view the effectiveness of steel reinforcement, only sample of the predicted results is presented here. The variation of axial stress for longitudinal bar at mid depth

along the span of the beam B4 at different stages of loading is shown in Fig. 8, where each element length is 50 mm. The chosen torques are 31.5, 32 and 37 kN.m which is only 0.5 kN.m less than failure torque (37.5 kN.m). Figure 9 shows the same but for stirrups (spaced at 150 mm, except the last 3 stirrups spaced at 50 mm) at mid depth of the beam. By scrutinizing these two figures, it can be noticed that up to the torque ($T_e = 31.5$ kN.m), which is more than the cracking torque (22 kN.m), the stresses in both longitudinal and transverse reinforcements is almost negligible, after that and due to the wide spread of the cracks along the span at $T = 32$ kN.m (Fig. 7), the steel stress suddenly increased and it has the same trend of distribution near the failure torque (37 kN.m). The variation of stresses for both types of reinforcement show that the peak stresses taken place at 450, 1200 and 1600 mm from fixed end and these may indicate the locations of formation of major cracks. None of the two types of reinforcement reached yield stress (400 Mpa).

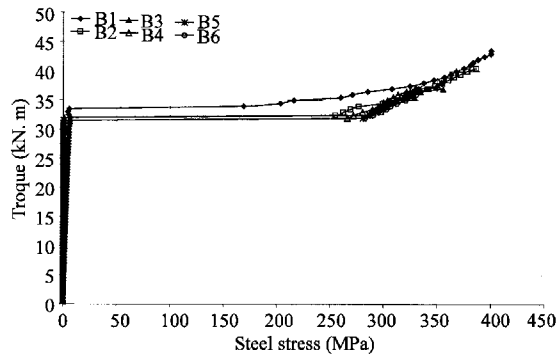


Fig. 10: Steel stress variation at different stages of loading up to failure

To trace the variation of steel stresses in all the beams during different stages of loading up to failure, the variation of stresses in the steel element that experienced maximum stress for all the beams are shown in Figure 10, which shows drastic increase of stress when the load exceeds the (T_e) value listed in Table 1. Figure 10 also shows that the steel stress in all the beams have never reached the yield stress except for beam B1 which sustained the largest ultimate torque (43.5 kN.m) and this is more than the design torque (23 kN.m) by 87%. The figure also shows that the stresses in steel in the beams are almost negligible until the torque exceeds the (T_e) value which is also more than cracking torque by 32-43% and more than the ACI318-05 design torque (23 kN.m) as well.

It is worth to mention that from the experimental work of Hao-Jan *et al.* (2006) for beams with transverse to longitudinal steel ratio $\rho_t/\rho_l = 1.0$ and total steel ratio $\rho_{total} = 1.0\%$, that the ratios of T_u/T_{cr} is about 1.32-1.59. In the present study the values of $\rho_t = 0.435$, $\rho_l = 0.452$, $\rho_{total} = 0.887\%$ and $\rho_t/\rho_l = 0.96$, the predicted T_u/T_{cr} ratios vary from 1.89 for beam B1 to 1.7 for beam B6 (Table 1) and considering the difference in the aspect ratio of the cross section of the beams and material properties used by Hao-Jan *et al.* (2006) and the present study, the predicted results can be considered fair enough compared with the experimental results by Hao-Jan *et al.* (2006), particularly for the beams with longer span.

CONCLUSIONS AND RECOMMENDATIONS

From the predicted results of the nonlinear analysis of reinforced concrete rectangular cantilever beams of different length, having same section and steel reinforcement subjected to pure torsion the following can be stated:

- The beams designed as per the ACI318-05 code to carry a factored torsion $T_u = 23$ kN.m, have shown a safety margin over the designed torsion equal to 89, 78, 67, 63, 63 and 63% for beams having span equal to 0.5, 1, 1.5, 2, 2.5 and 3 m, respectively. This shows the importance of the beam length, which are normally not taken into consideration in the design procedure.
- The maximum cracking torque, elastic limit torque and ultimate torque are predicted for the beam (B1) which has the shorter span with span to depth ratio equal to (1), these values get reduced with increasing the span and become constant when the span to depth ratio is equal to or more than (4) for this particular beam. This may be attributed to the effect of St. Venant principle.
- The stresses in the longitudinal and transverse reinforcements remain negligible even after the initiation of cracks and these stresses drastically increased after the wide spread of the cracks along the beam length. The steel attained yielding only in beam B1 (with shorter span) at a very high torque (43 kN.m), which is almost double the design torque.
- The predicted torsional stiffness for beam B1 with span to depth ratio equal to unity is 50 percent more than that of the elastic beam theory; while that of beam B6 with span to depth ratio equal to 6 the difference is only 7 percent, so the author suggests including the torsional stiffness of the reinforced concrete beam in the procedure for design of reinforced concrete beam for torsion.
- There is a need to carry out more rigorous study to separately investigate the effectiveness of each type of the torsional reinforcement of reinforced concrete beams subjected to pure torsion by varying the ratio of each type and to predict which type is more effective.
- The limitations of the present study are that the beam cross section and torsional reinforcement are kept constant. So more work are needed to study the effect of varying these parameters.

REFERENCES

- (ACI 318-05) and Commentary (ACI 318R-05), 2005. American Concrete Institute, Building Code Requirements for Reinforced Concrete, Farmington Hills.
- ANSYS-V10, 2005. ANSYS. Release 10.0, Copy right, SAS IP, Inc.
- Aryal, M.P., 2005. Longitudinal Reinforcement in Concrete Beams in Torsion. Application of Codes, Design and Regulations. Proceeding International Conference, Dundee, UK, 5-7 July, Ravindra K., D. Moray and A. Whyte (Eds.). Thomas Telfor, pp: 579-586.

- Desayi, P. and S. Krishnan, 1964. Equation for stress strain curve of concrete. *ACI J.*, 61: 345-350.
- Fang, I.K. and J.K. Shiau, 2004. Torsional behavior of normal and high-strength concrete beams. *ACI Struct. J.*, 101: 304-313.
- Hao-Jan, C., I.K. Fang, W.T. Young and J.K. Shiau, 2006. Behavior of Reinforced Concrete Beams with Minimum Torsional Reinforcement. *Eng. Stru.*, (In Press).
- Hsu, T.T.C., 1968. Ultimate Torque of reinforced concrete beams. *J. Struct. Div. ASCE*, 94: 485-510.
- Mac-Gregor, J.G., 1992. *Reinforced Concrete Mechanics and Design*. Prentice-Hall, Inc., Englewood Cliffs, NJ.
- Rahal, K.N., 2000. Torsional strength of reinforced concrete beams. *Can. J. Civ. Eng.*, 27: 445-453.
- William, K.J. and E.D. Warnke 1975. Constitutive model for the triaxial behavior of concrete. *Proceeding Int. Assoc. Bridge and Structural Engineering, ISMES, Bergamo, Italy*, 19: 174.
- William, K. and T.A. Tanabe 2001. *Finite Element Analysis of Reinforced Concrete Structures*. American Concrete Institute, Farmington Hills, MI.